J Mater Sci (2008) 43:2721–2730
DOI 10.1007/s10853-008-2449-9

Purification of lanthanum and cerium by plasma arc zone melting

Kouji Mimura · Takanori Sato · Minoru Isshiki

Received: 18 September 2007 / Accepted: 4 January 2008 / Published online: 21 February 2008

Abstract Purification of La and Ce by a horizontal plasma arc-zone melting (PZM) with Ar plasma arc heating under atmospheric pressure was examined. A stable molten zone of La and Ce on the water-cooled copper hearth could be maintained and, after zone passes, the segregation of impurities along the bars was recognized. Metallic impurities such as Fe, Cu, Al, and Si moved in the zone direction and decreased efficiently at the head side of the zone-melted bars. Especially, remarkable segregations of those impurities were observed on La. In addition, volatile impurities such as Ca, Mg, Zn, and Mn were reduced to further low levels by vaporization. For non-metallic impurities, O, N, C, and S in Ce, and O and N in La moved in the opposite direction of zoning, while C and S in La moved in the zone direction. Furthermore, nonmetallic impurities were reduced unexpectedly along the whole bar during PZM. Consequently, the purity around the head side of La and Ce bars could be sufficiently increased with PZM.

Introduction

The interests in rare earth metals, their alloys, and compounds have been raised from the needs in the advanced technology fields. Recently, rare earth metal oxides such as La_2O_3 and CeO_2 have been reported to be a promising candidate for high-k gate insulator films for the fabrication of scaled-down metal-oxide-semiconductor field effect transistor (MOS-FET) devices, due to their high dielectric constants and high stability with a Si surface [1–4]. For the use, high purity La and Ce metals would be required to improve the reliability and the lifetime of devices. For instance, some trace impurities might cause an increase in the gate leakage current. Hence, it is very important to reduce the impurity levels as low as possible.

However, the purities of commercial pure La and Ce metals are about 98–99 mass% at the most and they contains a large amount of metallic impurities (the other rare earth elements and Fe, Cu, Si, Al, Ca, etc.) and interstitial impurities, such as O, N, and C, because it is difficult to remove those impurities to low concentration levels, due to very high reactivity of rare earth metals. Therefore, more efficient and practical refining methods for La and Ce metals have been required recently.

For this purpose, solid-state electrotransport (SSE) and zone melting have been reported to be available for purification of Ce and La [5–8], since they have low vapor pressures at the respective melting point. The SSE is known to be useful for the redistribution of interstitial impurities but not of metallic (substantial) impurities and the yield is extremely low. On the other hand, the zone refining is expected to be good for the segregation of metallic impurities and to be developed as a practical purification method for rare earth metals, because it is much quicker and higher yield. However, the zone refining effect reported for La and Ce has been insufficient and the effectiveness is still obscure.

For example, Mimura et al. [9] refined La using electron-beam floating zone melting (EBFZM), and revealed that C moved in the zone direction, while S moved in the opposite direction and Ca and Mg could be removed by vaporization. However, there was no information on the

K. Mimura (✉) · T. Sato · M. Isshiki
Institute of Multidisciplinary Research for Advanced Materials, Tohoku University, 1,1 Katahira, 2-Chome, Aoba-ku, Sendai 980-8577, Japan
e-mail: mimura@tagen.tohoku.ac.jp

segregation of metallic impurities such as Fe, Cu, and Al, in addition, EBFZM is not a practical method due to the low productivity.

Fort et al. [10] examined a horizontal zone melting of Ce and La bars using r.f. heating (RF-ZM). Due to the high reactivity of rare earth metals, most of the materials (e.g., quarts, alumina, Ta, and BN) used at high temperatures were not applicable as a container of Ce and La during zone refining. Hence, they developed a "cold-boat" composed of six segments, each segment being a water-cooled rectangular copper tube. The segments were arranged in an approximately semicircular pattern with an internal diameter of about 10 mm, the gap between segments being about 1 mm. This gap is needed for heating a sample bar in the boat by induction heating.

They zone-refined Ce (15 passes at about 2 mm/min) in 0.1 MPa Ar atmosphere and revealed that O and N in Ce moved in the zone direction but no comment about the redistribution of metallic impurities. On the other hand, after zone refining of La (25 passes at 2–3 mm/min) in high vacuum, they observed that metallic impurities such as Fe, Cu and Ni moved in the zone direction but their segregation degrees were not so large. In addition, the segregation of O and N was not observed clearly. An uncertainty in the segregation effect observed in the RF-ZM is probably caused by an unstable molten zone of La in the "cold-boat" under vacuum, as described in the literature.

On the other hand, from the phase diagrams of La- and Ce-binary alloys [11], the distribution coefficients of many metallic impurities such as Al, Ca. Cu, Fe, and Si in La and Ce are estimated to be considerably smaller than unity. Therefore, those metallic impurities must be segregated to the tail end, when a stable molten zone could be formed during the zone melting. Hence, in the present work, we examined the zone refining of La and Ce using plasma-arc heating, this method which was developed by the authors and called plasma-arc-zone melting (PZM). By PZM, purifications of Si and Cr have already investigated and the good refining results have been obtained [12, 13], in which the formation of a stable molten zone by plasma arc heating has been observed.

Experimental procedure

Commercial pure La and Ce were used as the starting materials and the main impurity concentrations of both metals, analyzed by GDMS, are indicated in Table 1. Besides rare earth metal impurities (about 220 and 250 mass ppm, in total, contained in La and Ce, respectively), large amounts of metallic impurities such as Al, Fe, Cu, and Si were contained from nearly 50 mass ppm to 500 mass ppm and, furthermore, large amounts of non-metallic impurities such as O, N, C, and S were contained about 500–5000 mass ppm.

Table 1 Impurity concentrations (mass ppm) of Ce and La as the starting materials

Impurity	La	Ce
Mg	3.7	2.4
Al	70	500
Si	70	350
Ca	450	40
Fe	160	400
Mn	0.8	3
Ni	2	3
Co	4	2
Cu	360	270
Zn	25	13
Y	10	30
Ce	48	–
La	–	68
Pr	0.6	6
Nd	14	38
Tb	2	5
Gd	180	70
C	1,900	570
N	930	510
O	4,800	1,600
S	5,000	1,200

Figure 1 shows the schematic diagram of PZM apparatus used in this work. A d.c. arc-discharged type plasma torch with a maximum power of 20 kW is equipped on a stainless steel vessel (200 mmW × 800 mmL × 180 mmH). Pure Ar gas, as a plasma generating gas, is introduced into the plasma torch at a flow rate of 5 L/min. The specimen bar is placed on the groove (20 mmW × 200 mmL, 5 mm in depth) cut in the water-cooled copper hearth (40 mmW × 240 mmL × 40 mmH), which is movable horizontally at a constant speed of 0.1–10 mm/min.

Primary bars of La and Ce (25–28 g of mass, about 15 mm in diameter and 65–70 mm in length) were at first prepared by arc melting under 0.1 MPa Ar atmosphere. Three primary bars were then placed in a row on the copper hearth and welded by Ar plasma-arc heating to make a La bar and a Ce bar (approximately 75–80 g of mass, about 15 mm in diameter and 200 mm in length) as the starting material for the following PZM treatment. The power of Ar plasma-arc for PZM was set at about 3.4 kW. A stable molten zone, about 25–30 mm in length, could be formed by Ar plasma arc heating and the horizontal zone melting of Ce and La bars was carried out by moving the hearth at a constant speed of 3 mm/min. This means the zoning speed of 3 mm/min. The zone-melted bar should be turned over after each pass, because the bottom in contact with the copper hearth was not melted. Then, the number of zone

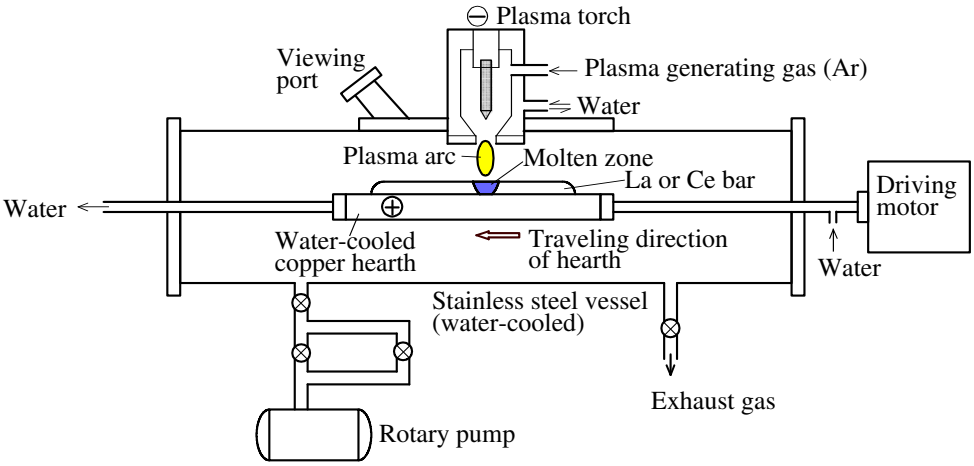

Fig. 1 Schematic diagram of plasma arc zone melting (PZM) apparatus

passes was consequently set to be even number from 2 to 20.

The La and Ce bars after PZM were divided into five equal parts and the center of each part was analyzed. Specimens for analysis were rolled to discs in shape with about 20 mm in diameter and nearly 1 mm in thickness, followed by mechanically polished and rinsed in ethanol. All metallic and non-metallic impurities, except hydrogen and rare gases, were analyzed by a glow-discharge mass spectrometer (GDMS).

Results and discussion

PZM of La

The Fe, Cu, Al, Si, and Ca concentration profiles along the La bars after 2–20 passes of PZM at 3 mm/min and their initial concentrations before PZM are shown in Figs. 2–6, respectively. The abscissa by *x/L* indicates the fractional distance, in which *x* and *L* represent the distance from the head edge of the bar and the total length, respectively.

As seen in Fig. 2, Fe moved in the zoning direction and the segregation was clearly observed with the increase in the number of passes, although it was not clear at 2 passes. Then the Fe concentration decreased to below 1 mass ppm at the head side and increased to nearly 300 mass ppm at the tail side after 20 passes. It was realized, therefore, that a sufficient segregation effect proceeded during PZM and it was superior to that during RF-ZM.

Similar result was obtained for Cu as shown in Fig. 3. The Cu concentration decreased to about 1 mass ppm at the head side and increased to about 1,000 mass ppm at the tail side after 20 passes. Fort et al. [10] observed the same tendency of Cu after RF-ZM of La, but the segregation degree of Cu was considerably lower than that of the present work on PZM. Figure 7 shows the C/C_o profiles along the zone melted La bars (C: Cu concentration at each

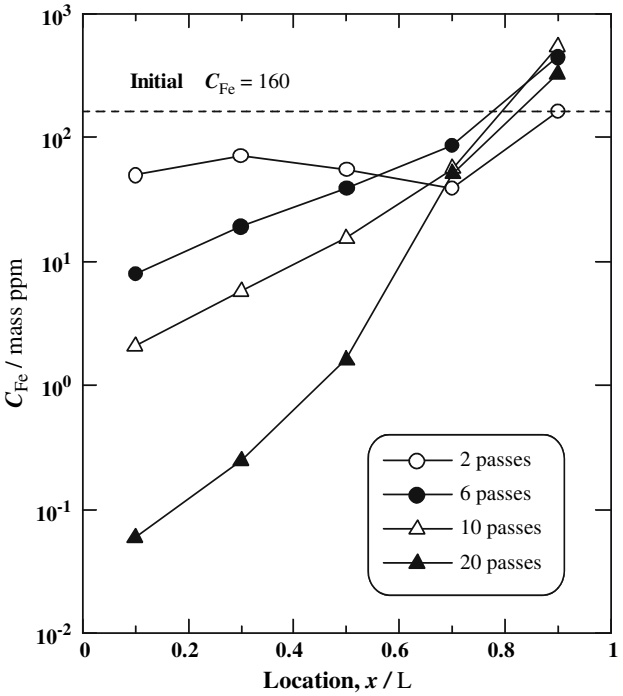

Fig. 2 Fe concentration profiles along La bars after 2–20 passes of plasma arc zone melting at 3 mm/min

position, C_o: the initial Cu concentration) of both PZM at 20 passes (Fig. 3) and RF-ZM at 25 passes, in order to compare the segregation effect of PZM with that of RF-ZM. In the case of RF-ZM, the Cu concentration along the whole bar increased above the initial concentration and the redistribution of Cu was not clear, although the initial concentration ($C_o = 4$ mass ppm) was considerably smaller than that of this work. This would be probably caused by a contamination of the La bar with Cu from the copper "cold-boat," due to its insufficient cooling power. It should be noted, on the other hand, that no contamination with Cu was found on PZM and a good segregation of Cu along the bar was recognized.

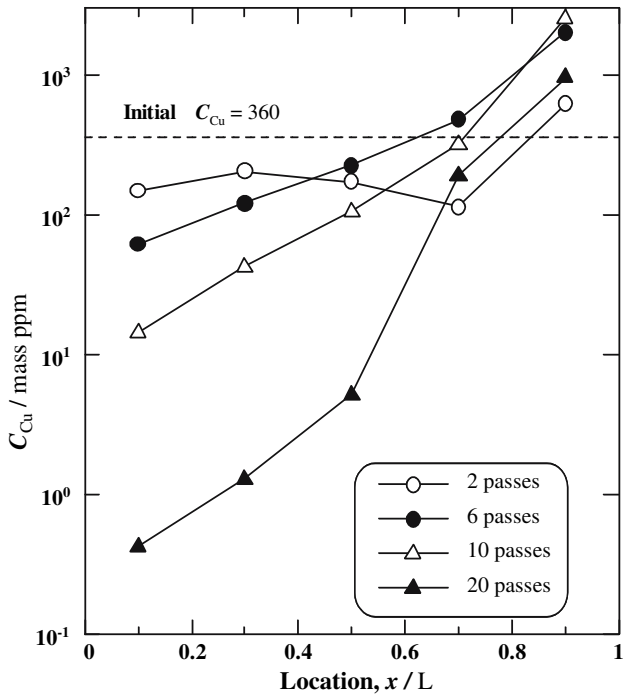

Fig. 3 Cu concentration profiles along La bars after 2–20 passes of plasma arc zone melting at 3 mm/min

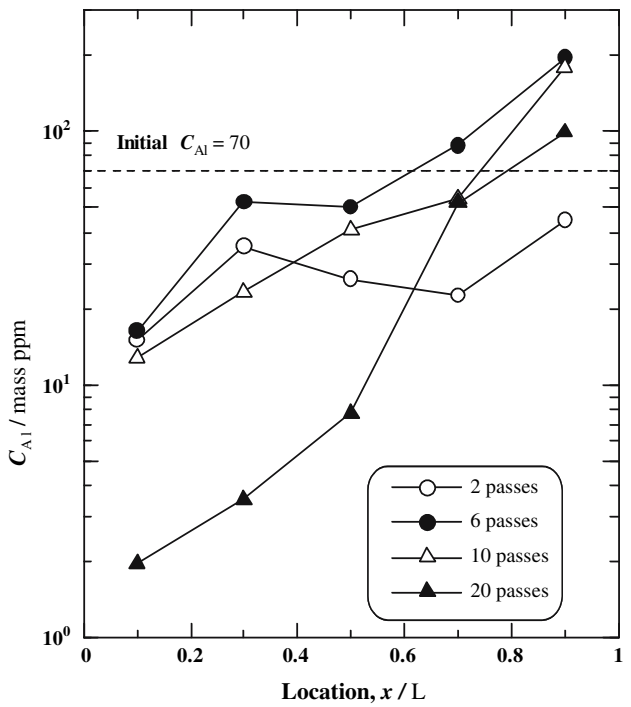

Fig. 4 Al concentration profiles along La bars after 2–20 passes of plasma arc zone melting at 3 mm/min

For Al and Si, they also concentrated at the tail end and segregated like Fe and Cu as shown in Figs. 4 and 5. After 20 passes, the concentration of Al and Si decreased to below 10 and below 1 mass ppm, respectively.

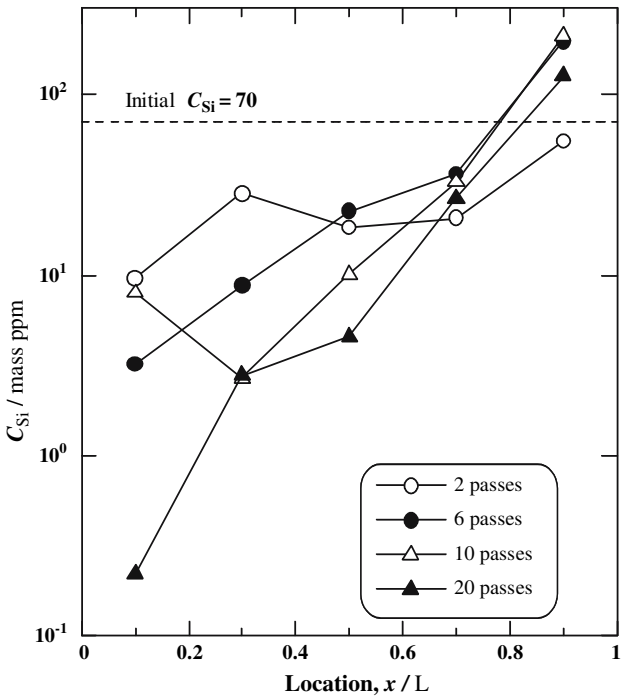

Fig. 5 Si concentration profiles along La bars after 2–20 passes of plasma arc zone melting at 3 mm/min

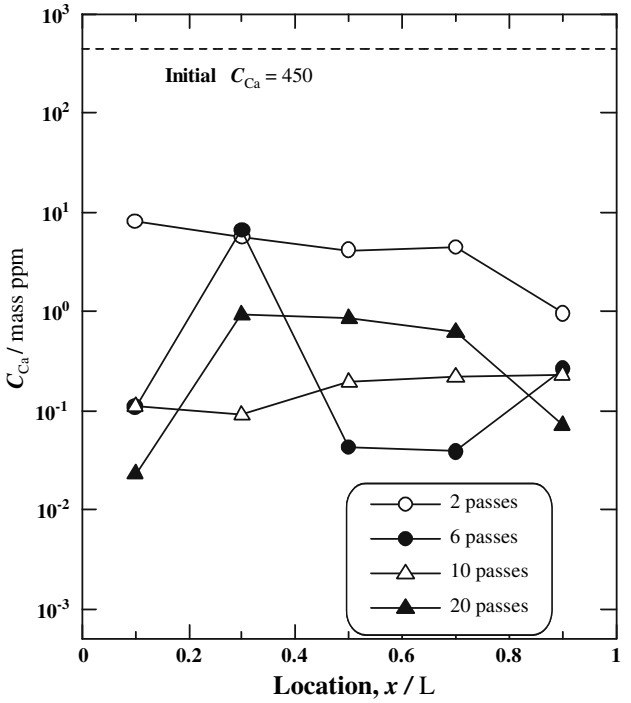

Fig. 6 Ca concentration profiles along La bars after 2–20 passes of plasma arc zone melting at 3 mm/min

On the other hand, it can be seen in Figs. 6 and 7 that the Ca concentration in the whole bar decreased to below 1 mass ppm after 10 passes. Similar results were obtained

for Mg and Zn and both of them decreased to less than 1 mass ppm after 10 passes. The results suggested that these metallic impurities with fairly higher vapor pressures than that of La, as shown in Fig. 8, must be eliminated by vaporization from the molten La zone during PZM.

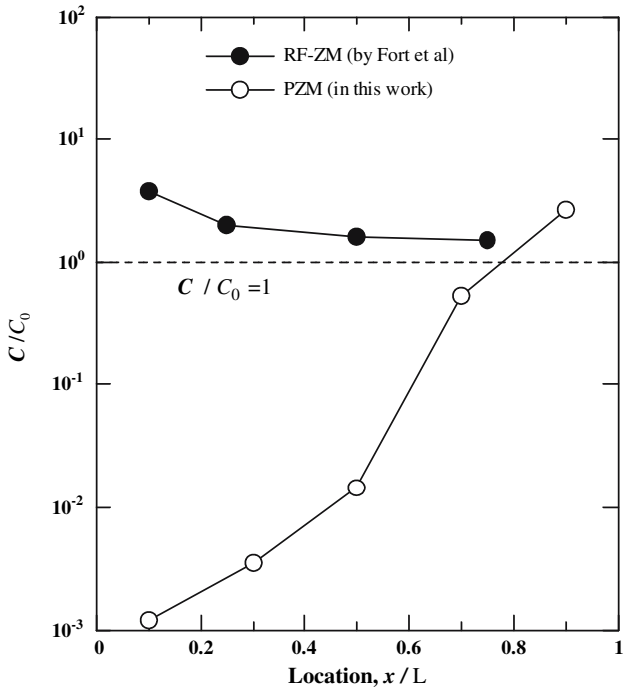

Fig. 7 Comparison of Cu concentration profiles (C/C_0) along the zone melted La bar by PZM (after 20 passes at 3 mm/min) with that by RF-ZM (25 passes at about 2–3 mm/min) [C: Cu concentration at each position, C_0: Initial Cu concentration]

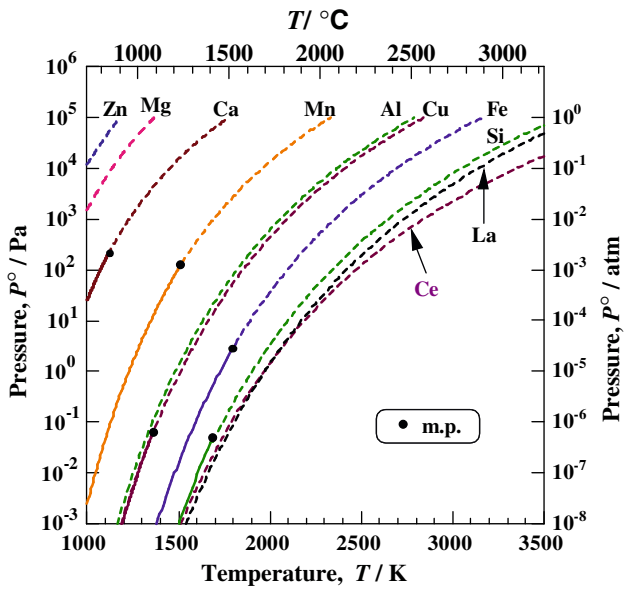

Fig. 8 Vapor pressures of Ce, La and several related metal elements as a function of temperature

Figures 9–12 shows the O, N, C and S concentration profiles along the zone melted La bars after 2–20 pass of PZM and the initial concentrations before PZM, respectively. In Figs. 9 and 10, O and N moved slightly in the

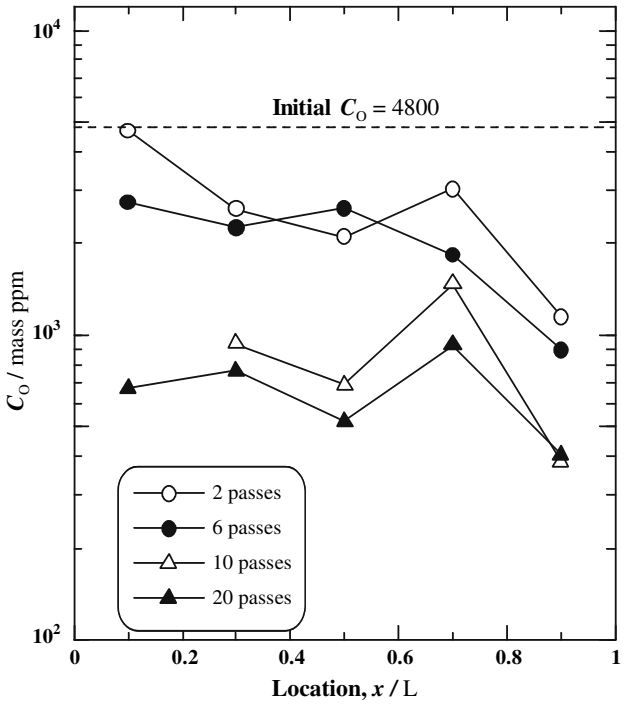

Fig. 9 Oxygen concentration profiles along La bars after 2–20 passes of plasma arc zone melting at 3 mm/min

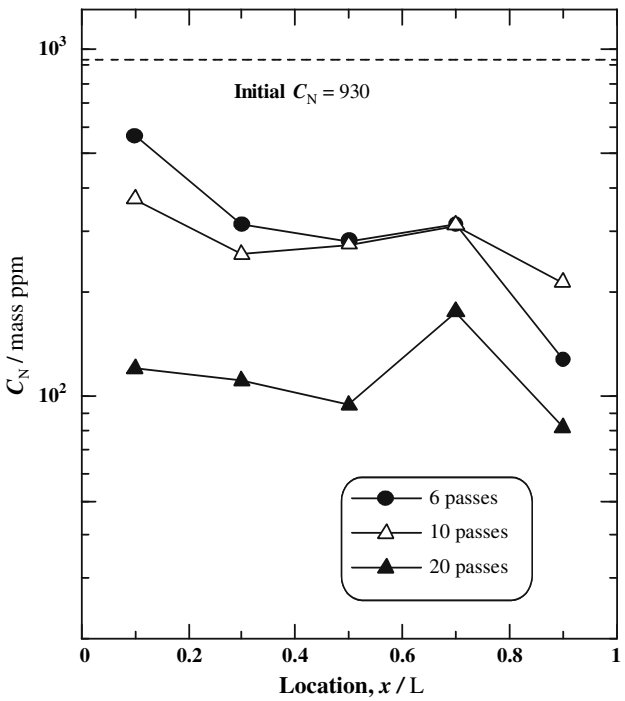

Fig. 10 Nitrogen concentration profiles along La bars after 2–20 passes of plasma arc zone melting at 3 mm/min

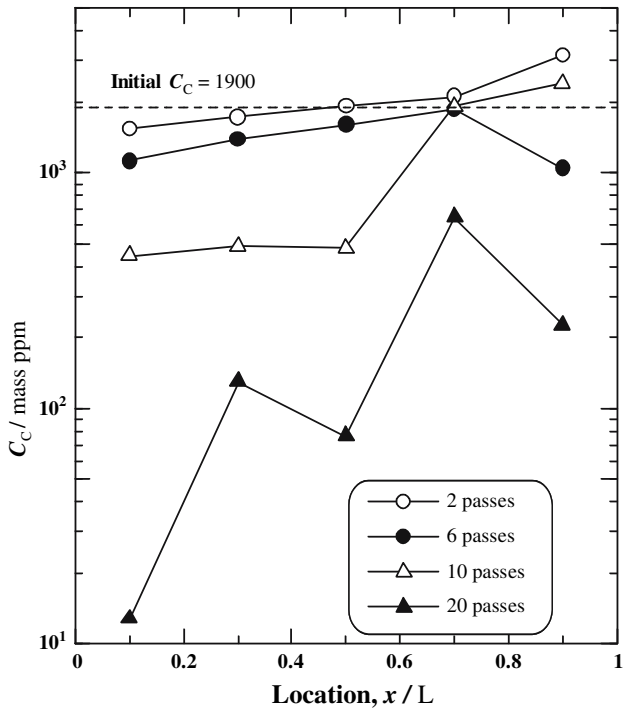

Fig. 11 Carbon concentration profiles along La bars after 2–20 passes of plasma arc zone melting at 3 mm/min

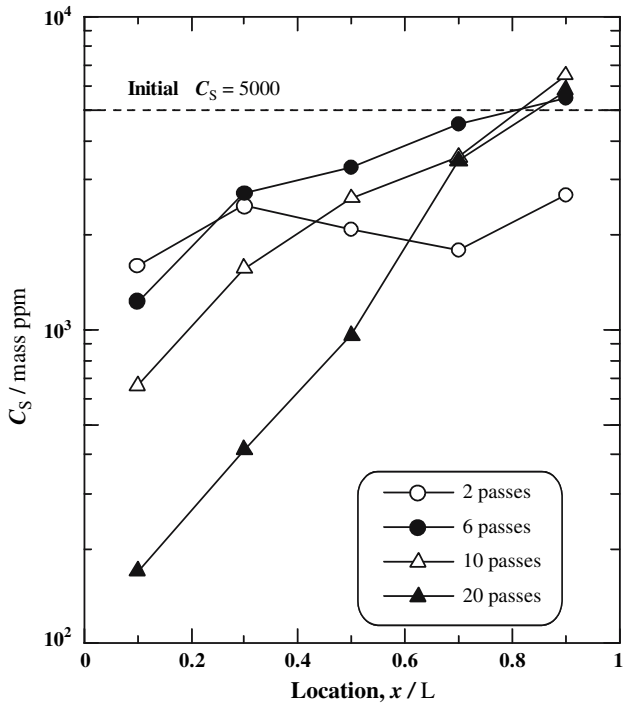

Fig. 12 Sulfur concentration profiles along La bars after 2–20 passes of plasma arc zone melting at 3 mm/min

opposite direction to zoning, which were the same as the results obtained on the RF-ZM of La. In addition, they decreased gradually along the whole La bar with the number of passes. Consequently, O and N at the tail end could be lowered nearly 400 and 100 mass ppm, respectively, which were about one tenth of those initial concentrations.

It is known to be very difficult to remove O and N from La and Ce, since there are strong affinities between rare earth metals and nonmetallic impurities [14]. However, the decreases in O and N were clearly observed during PZM and the causes for it are not clear at present. Therefore, PZM is thought to be an attractive method for the removal of O and N from La. For the deoxidation, an increase in the surface temperature of molten zone heated by Ar plasma arc may enhance the vaporization of oxides such as SiO, Al_2O, and CO from the La molten zone. In order to make it clear, further examination will be needed.

On the other hand, C and S moved in the zone direction, as shown in Figs. 11 and 12, which were the same results obtained in the EBFZM of La. Especially, the excellent segregation of sulfur (Fig. 12) was observed clearly. Hence, C and S could be lowered with the number of passes and decreased below 100 and 200 mass ppm, respectively, at the head side after 20 passes.

It is realized, therefore, that the distribution coefficients of C and S in La are less than unity, while those of O and N are more than unity.

PZM of Ce

The Fe, Cu, and Ca concentration profiles along the Ce bars after 2–20 passes of Ar-PZM at 3 mm/min and their initial concentrations before PZM are shown in Figs. 13–15, respectively.

As seen in Fig. 13, Fe moved in the zone direction and the segregation was obviously observed with the increase in the number of passes, although it was not clear at 2 passes. In addition to the segregation, the total Fe content was certainly reduced to a lower level than the initial content as the number of pass increased. This was probably caused by the vaporization of Fe from the molten Ce zone, due to a higher vapor pressure of Fe than that of Ce as indicated in Fig. 8. Thus, the Fe concentration at the head side could be reduced to nearly 100 mass ppm at 10 passes and below 50 mass ppm at 20 passes. In the same way, Cu (Fig. 14), Al and Si moved to the tail side and vaporized with the number of pass and decreased below 50, nearly 100 and below 50 mass ppm, respectively, at the head side after 20 passes. However, the degrees in segregation of Al and Si were somewhat smaller than that of Fe. These results agree with the distribution coefficients estimated from the respective phase diagrams of Ce binary alloys.

On the other hand, it can be seen in Fig. 15 that Ca in the whole bar markedly decreased to below 1 mass ppm at

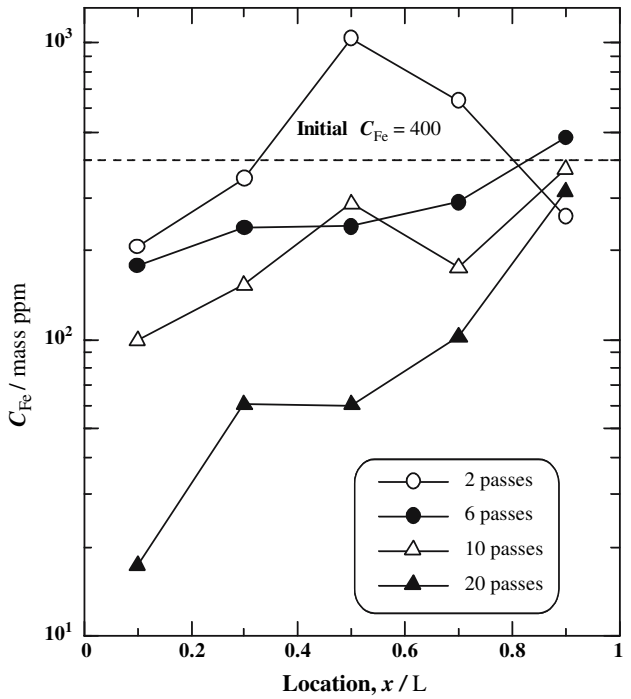

Fig. 13 Fe concentration profiles along Ce bars after 2–20 passes of plasma arc zone melting at 3 mm/min

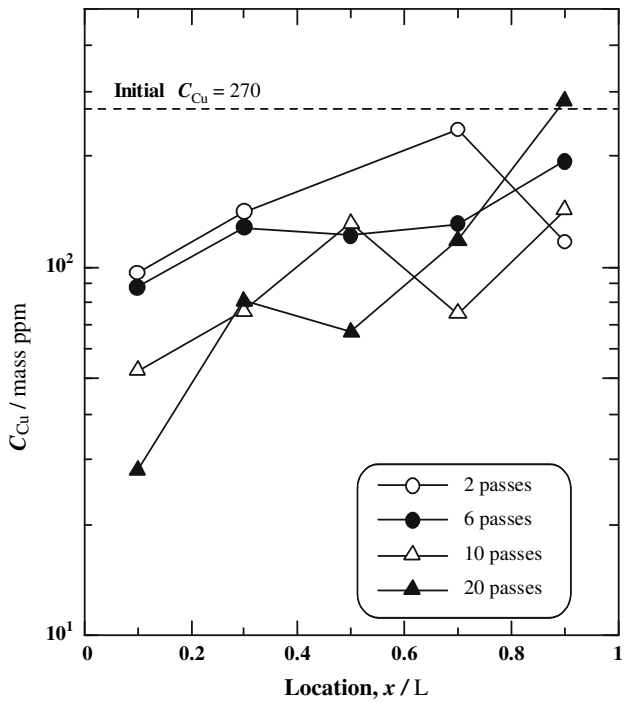

Fig. 14 Cu concentration profiles along Ce bars after 2–20 passes of plasma arc zone melting at 3 mm/min

10 passes and to below 0.1 mass ppm at 20 passes, besides a slight progress of the segregation. Similar results were obtained for Mg and Zn, and they decreased to less than 0.1 mass ppm at 10 passes. These metallic impurities with

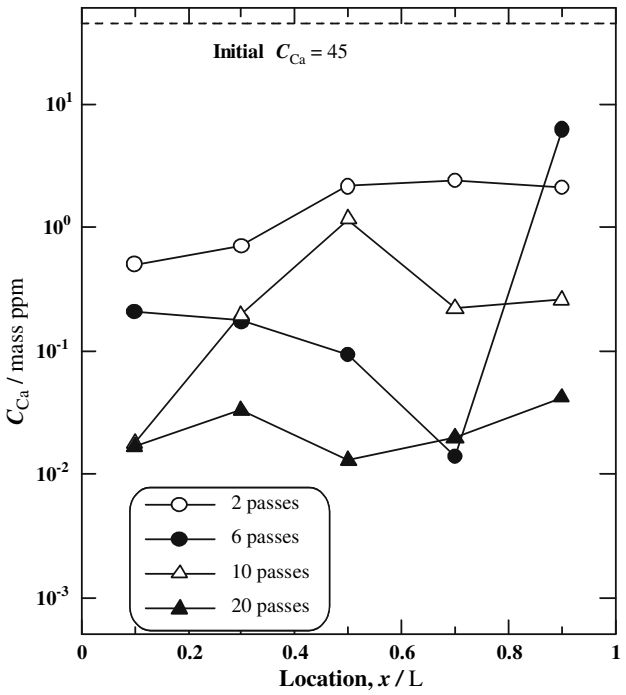

Fig. 15 Ca concentration profiles along Ce bars after 2–20 passes of plasma arc zone melting at 3 mm/min

higher vapor pressures than that of Ce as presented in Fig. 8, therefore, must be eliminated by vaporization from the molten zone.

The O, N, C, and S concentration profiles along the zone melted Ce bars after 6–20 passes and their initial concentrations before PZM are shown in Figs. 16–19, respectively.

Segregations of O, C, N, and S along the bars were observed, although there were somewhat spreads of values, and their concentrations were exactly to be lowered around the tail side with increasing in the number of passes. Their distribution coefficients are estimated to be a little higher than unity, which are the same as the results of O and N in the zone-melted Ce by RF-ZM [10]. Furthermore, it was found in present work that all of them gradually decreased along the whole bar with the number of passes, as the earlier-mentioned results of La. Consequently, they could be reduced from the initial concentrations to considerably lower levels around the tail side after more than 10 passes; from 1,600 to below 100 mass ppm for oxygen, from 510 to nearly 10 mass ppm for nitrogen, from 570 to below 100 mass ppm for carbon, and from 1,200 to below 500 mass ppm for sulfur.

Purity of Ce and La before and after PZM

Tables 2 and 3 indicate the concentrations of metallic and non-metallic impurities of La and Ce before and after 20

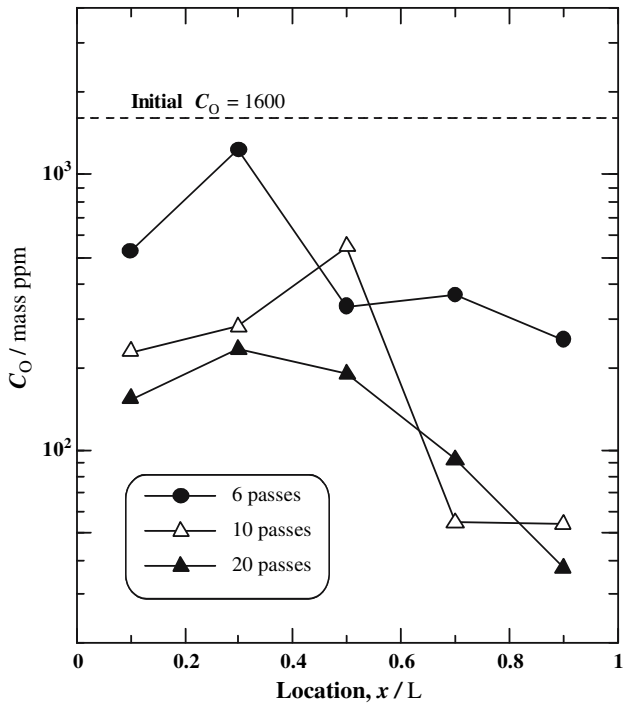

Fig. 16 Oxygen concentration profiles along Ce bars after 6–20 passes of plasma arc zone melting at 3 mm/min

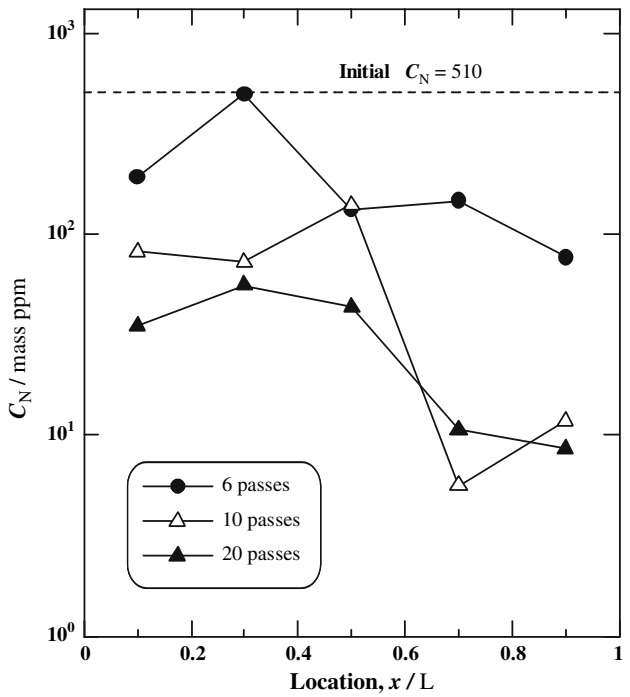

Fig. 17 Nitrogen concentration profiles along Ce bars after 6–20 passes of plasma arc zone melting at 3 mm/min

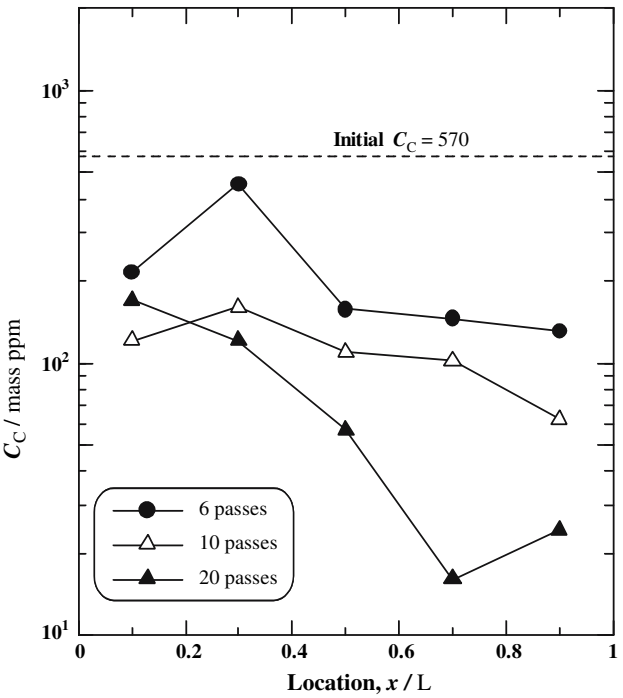

Fig. 18 Carbon concentration profiles along Ce bars after 6–20 passes of plasma arc zone melting at 3 mm/min

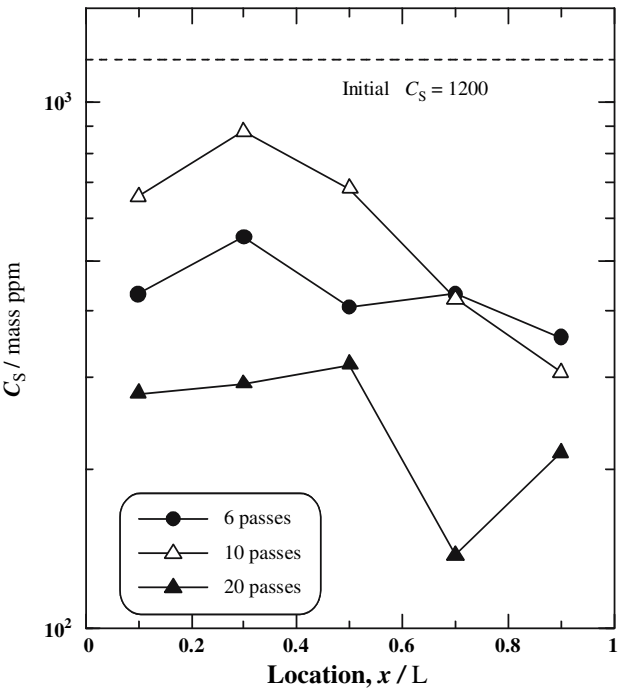

Fig. 19 Sulfur concentration profiles along Ce bars after 6–20 passes of plasma arc zone melting at 3 mm/min

passes of PZM. In the case of "after PZM", the values in both the head sides (x/L = 0.1) and the tail sides (x/L = 0.9) of La and Ce bars are represented, respectively. As would be anticipated, no segregation and no reduction of rare earth metal impurities like Ce, Nd, and Gd in La and like La, Nd, and Gd in Ce were observed.

On the other hand, many metallic impurities, except rare earth metals, such as Al, Si, Fe, Cu, Ni, and Co were

Table 2 Analyses of La staring material and after 20 passes of PZM, in which the impurity concentrations (mass ppm) are indicated at the head side ($x/L = 0.1$) and at the tail side ($x/L = 0.9$)

Impurity	Starting material	After 20 passes	
		$x/L = 0.1$	$x/L = 0.9$
Mg	3.7	0.02	0.01
Al	70	2	100
Si	70	0.2	130
Ca	450	0.02	0.1
Fe	160	0.1	320
Mn	0.8	0.04	1
Ni	2	0.05	5
Co	4	0.001	8
Cu	360	0.4	960
Zn	25	0.07	0.1
Y	10	3	3
Ce	48	48	45
Pr	0.6	0.5	0.6
Nd	14	14	13
Tb	2	2	1
Gd	180	180	140
C	1,900	450	2,400
N	930	120	80
O	4,800	670	400
S	5,000	170	5,800

Table 3 Analyses of Ce staring material and after 20 passes of PZM, in which the impurity concentrations (mass ppm) are indicated at the head side ($x/L = 0.1$) and at the tail side ($x/L = 0.9$)

Impurity	Starting material	After 20 passes	
		$x/L = 0.1$	$x/L = 0.9$
Mg	2.4	0.002	0.03
Al	500	65	170
Si	350	18	120
Ca	40	0.02	0.04
Fe	400	20	320
Mn	3	0.3	0.7
Ni	3	0.2	3
Co	2	0.2	3
Cu	270	30	280
Zn	13	0.01	0.01
Y	30	7	5
La	68	68	61
Pr	6	7	8
Nd	38	38	30
Tb	5	5	4
Gd	70	55	49
C	570	120	62
N	510	35	9
O	1,600	150	38
S	1,200	660	300

segregated in the zone direction and exactly decreased at the head sides of both La and Ce bars, as mentioned earlier and as expected from the corresponding phase diagrams of Ce- and La-binary alloys. Especially, a marked segregation effect of PZM on La bars has obviously been recognized. Moreover, another metallic impurities with considerably higher vapor pressures than those of Ce and La, such as Ca, Mg, Zn, and Mn, could be lowered to the very low concentration levels, probably by vaporization.

For nonmetallic impurities, such as O, N, C, and S of Ce, all of them moved in the opposite direction for zoning and decreased at the tail side. On the other hand, in the case of La, O, and N moved in the opposite direction to zoning but C and S moved in the zone direction.

Consequently, the purity in the head side of La bar after 20 passes of PZM, which is estimated from the sum of all metallic and non-metallic impurity concentrations, increased to above 99.8 mass% from 98.6 mass% of the initial purity and that of Ce also increased to above 99.8 mass% from 99.4 mass% of the initial purity.

From the above-mentioned refining results of La and Ce by PZM, the increase in the number of zone passes was very useful to enhance the segregation of many impurities, but it needed a lot of efforts. It is supposed, on the other hand, that the same refining results could be accomplished without increasing the number of passes, when the zoning speed was lowered, for example, from 3 mm/min to 1 mm/min.

Conclusions

Purification of Ce and La with plasma-arc-zone melting (PZM) was examined. Since a stable molten zone of Ce and La on the water-cooled copper hearth could be maintained by Ar plasma arc heating, the effect of zone melting on the segregation of impurities along Ce and La bars was exhibited clearly.

For metallic impurities, Fe, Cu, Al, and Si moved in the zone direction and decreased efficiently around the head side of the zone-melted bars. Especially, remarkable segregations of those impurities was observed on PZM of La bars. In addition, volatile impurities such as Ca, Mg, Zn, and Mn were reduced to low levels by vaporization during the PZM.

For nonmetallic impurities, in the case of Ce, O, N, C, and S moved in the opposite direction for zoning and decreased at the tail side. In the case of La, O, and N moved in the opposite direction for zoning but C and S moved in the zone direction. Furthermore, O, N, C, and S

of Ce, and O and N of La could be reduced in the whole bar during PZM, although the refining mechanism has been unknown.

Therefore, PZM has been realized to be a very useful and practical purification method for La and Ce. It is also expected to be effective on purification of the other rare earth metals such as Pr, Nd, Gd and Tb, which have low vapor pressures at each melting point as well as La and Ce.

Acknowledgements The authors are grateful to Nano-Technical Laboratory of IMRAM (Institute of Multidisciplinary Research for Advanced Materials), Tohoku University for the technical support to GDMS operation. This work was financially supported by a Grant-in-Aid for Scientific Research (B) from Japan Society for the Promotion of Science (JSPS) and by a Feasibility Study from Japan Science and Technology Agency (JST).

References

1. Maria JP, Wicaksana D, Kingon AI, Bush B, Schulte H, Garfunkel E, Gustafsson T (2001) J Appl Phys 90:3476
2. Wu X, Landheer D, Sproule GI, Quance T, Graham MJ, Botton GA (2002) J Vac Sci Technol A 20:1141
3. Joumori S, Nakajima K, Suzuki M, Kimura K, Nishikawa Y, Matsushita D, Yamaguchi T, Satou N (2004) Jpn J Appl Phys 43:7881
4. Nishikawa Y, Fukushima N, Yasuda N, Nakayama K, Ikegawa S (2002) Jpn J Appl Phys 41:2480
5. Gupta CK, Krishnamurthy N (2005) In: Extractive metallurgy of rare earths, CRC Press, Boca Raton, p 291
6. Gupta CK, Krishnamurthy N (1992) Int Mater Rev 37:197
7. Gschneider KA Jr (1993) J Alloys Comp 193:1
8. Fort D (2001) In: Purification process and characterization of ultra high purity metals. Springer-Verlag, Berlin, p 145
9. Mimura K, Isshiki M (1993) In: Henein H, Oki T (eds) Proceedings of 1st international conference on processing materials for properties, Hawaii, Nov. 1993. The Minerals, Metals and Materials Society (TMS), p 897
10. Fort D, Jones DW, Beaudry BJ, Gschneider KA Jr (1981) J Less-Common Metals 81:273
11. Massalski TB, Okamoto H, Subramanian PR, Kacprzak L (1990) In: Binary alloy phase diagrams, 2nd edn. ASM International
12. Mimura K, Isshiki M (2005) Metals Mater Process 17:31
13. Mimura K, Komukai T, Isshiki M (2005) Mater Sci Eng A 403:11
14. Okabe TH, Jacob KT, Waseda Y (2001) In: Purification process and characterization of ultra high purity metals. Springer-Verlag, Berlin, p 3
15. Knacke O, Kubashewski O, Hesselmann K (1991) In: Thermochemical properties of inorganic substances, 2nd edn. Springer-Verlag, Berlin